Beyond the Linearized Stability Limit in Non Linear Problems

Conference Paper · July 1985

CITATIONS
20

READS
57

2 authors, including:

David F. Griffiths
University of Dundee
124 PUBLICATIONS **4,213** CITATIONS

SEE PROFILE

D F Griffiths & G A Watson (Editors)

University of Dundee

Numerical analysis

Longman Scientific & Technical

Copublished in the United States with
John Wiley & Sons, Inc., New York

A R MITCHELL & D F GRIFFITHS

Beyond the linearised stability limit in nonlinear problems

1. INTRODUCTION

In recent years a new type of "numerical analyst" has emerged. This is a person probably from physics or biology, equipped with a small computer, who carries out long time calculations with a fixed time step of non linear problems, the latter modelled either by differential or difference equations. Not for this person is a well behaved solution, unique at each point in space and time being sought, but more likely phenomena such as bifurcation, period doubling, chaos, recurrence etc. Most desirable of these is chaos where the solutions have stochastic behaviour even although the governing equations are deterministic. This has given fluid dynamicists a new hope of understanding the onset of turbulence in a viscous flow where the Reynolds Number parameter is being increased.

Non linear problems tend to be individual and in this paper we shall concentrate on two different examples of non linear instability and its effect on the respective solutions. The examples are taken from

(I) Mathematical Biology and the non linear terms $u(1-u)$.

(II) Dispersive waves and the Korteweg de Vries equation.

2. THE NON LINEAR TERM $u(1-u)$

2.1 Map on the line

In population dynamics, May [1] considered the difference equation model (or map on the line)

$$V_{n+1} = aV_n(1-V_n) , \quad n = 0,1,2,... \tag{2.1}$$

where $a(>0)$ is a parameter. If we put

$$V_n = \frac{\alpha k}{1 + \alpha k} U_n \quad \text{and} \quad a = 1 + \alpha k$$

into (2.1), we get

$$U_{n+1} = (1 + \alpha k)U_n - \alpha k U_n^2 \tag{2.2}$$

which is the forward Euler difference replacement of the equation

$$\frac{du}{dt} = \alpha u(1-u) , \qquad \alpha > 0 \tag{2.3}$$

where $\alpha(>0)$ is a parameter and $k(>0)$ is the time step. The solution $u = 1$ is a stable rest point of (2.3) and if we put

$$U_n = 1 + \epsilon_n$$

in (2.2), where ϵ_n is small, and linearise, $U = 1$ emerges as a stable rest point of (2.2) provided

$$0 < \alpha k \leq 2 . \tag{2.4}$$

Returning to May's notation, it follows that linearised stability is present about the asymptotic solution

$$V = \frac{a - 1}{a} \tag{2.5}$$

provided

$$1 < a \leq 3 . \tag{2.6}$$

A series of numerical experiments using (2.1) was carried out for a range of values of the parameter a, and the results shown in Figure 1. In each experiment, the initial condition was taken to be $U_0 = \frac{1}{2}$ and the iteration continued until the asymptotic (in time) solution was obtained. Period doubling started at $a = 3$ and continued until $a \doteqdot 3.57$ when chaos was encountered. If period 2^j, j an integer, occurs for the parameter a_j and $a_\infty = \lim_{j\to\infty} a_j$, then

$$\frac{a_\infty - a_j}{a_\infty - a_{j+1}} \to 4.6692 \quad \text{as} \quad j \to \infty ,$$

where 4.6692 is the Feigenbaum constant [2].

2.2 Map on the plane

The quadratic map introduced first by Hénon [3] is

$$\begin{aligned} x_{n+1} &= 1 - \mu x_n^2 + y_n , \\ y_{n+1} &= b x_n , \end{aligned} \qquad n = 0,1,2,\ldots \tag{2.7}$$

where μ and b are parameters. If we put

$$x = \frac{1}{\mu}[az - \tfrac{1}{2}(a+1-b)] \quad \text{and} \quad \mu = \tfrac{1}{4}[a^2 - (1-b)^2] \tag{2.8}$$

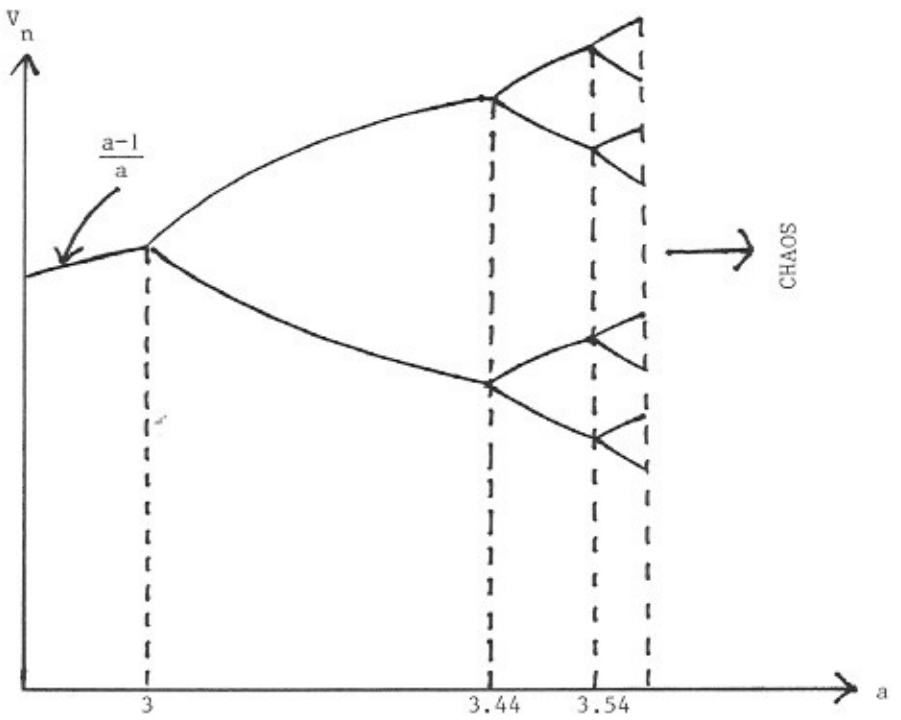

Figure 1. Period doubling leading to chaos

(2.7) reduces to

$$z_{n+1} = az_n(1-z_n) + (1-b)z_n + bz_{n-1}, \quad n = 1,2,3,\ldots . \tag{2.9}$$

If $a = 2\alpha k$ and $b = 1$, (2.9) reduces to

$$z_{n+1} = 2\alpha k z_n(1-z_n) + z_{n-1} \tag{2.10}$$

which is the leap frog (or mid point) difference replacement of (2.3). In the phase plane, z_{n+1} plotted against z_n, there are two unstable fixed points (0,0) and (1,1) and two period 2 points (1,0) and (0,1). Following Sanz-Serna [4] we rewrite (2.10) as the augmented system

$$\begin{aligned} u_{n+1} &= u_n + 2\alpha k v_n(1-v_n) \\ v_{n+1} &= v_n + 2\alpha k u_{n+1}(1-u_{n+1}) \end{aligned} \tag{2.11}$$

where $u_n = z_{2n}$ and $v_n = z_{2n+1}$, $n = 0,1,2,\ldots$. The system (2.11) in the phase plane, v_n plotted against u_n, has two unstable fixed points (0,0) and (1,1) and two neutrally stable fixed points (1,0) and (0,1) provided $\alpha k \leq 1$.

The qualitative behaviour of solutions of (2.11) and consequently (2.10) for small time steps may be deduced by observing that (2.11) is consistent with the augmented system

$$\frac{du}{dt} = \alpha v(1-v)$$

$$\frac{dv}{dt} = \alpha u(1-u)$$

which contains the solutions of (2.3) as the special case $u = v$. This system has the first integral

$$\tfrac{1}{2}u^2 - \tfrac{1}{3}u^3 = \tfrac{1}{2}v^2 - \tfrac{1}{3}v^3 + \text{constant}$$

from which it follows that the invariant curves are given by the diagonal $u = v$ and the ellipse

$$(u + v - 1)^2 + \tfrac{1}{3}(u-v)^2 = 1.$$

With initial values chosen inside this ellipse, the solutions describe orbits around the centres (0,1) and (1,0) while points outside the ellipse "blow up" along $u \sim v \to -\infty$ in finite time. These qualitative properties of the augmented system clearly describe the behaviour of the trajectories of (2.11) shown in Figure 2 for $\alpha k = 0.1$, and a variety of initial conditions. This has previously been noted by Sanz-Serna [4].

The solutions of (2.11) depend on the three parameters u_0, v_0 and αk. However, since (2.11) is, through (2.10), a difference replacement of (2.3), then u_0 and v_0 should not be treated as independent parameters but should be chosen so that the numerical solution follows the unstable manifold joining (0,0) to (1.1). For finite values of αk, this unstable manifold denoted by $v = \phi(u)$ is not linear but is smooth in the neighbourhood of the origin and can be expressed as the Taylor series

$$\phi(u) = a_1 u + a_2 u^2 + a_3 u^3 + \ldots$$

where $a_1 = \alpha k + (1 + \alpha^2 k^2)^{\frac{1}{2}}$,

$a_2 = 2\alpha k a_1^2/(2\alpha k - 1 - a_1 - 2\alpha k a_1)$

and $a_3 = 2a_1 a_2(2\alpha k + a_2)/(2\alpha k - a_1 - a_1^3)$.

As the unstable manifold approaches the saddle point (1,1) it oscillates with increasing frequency and amplitude and becomes wrapped around the orbital solutions neighbouring (1,0) and (0,1) while being bounded externally by the two unstable manifolds that extend from (1,1) to the origin. (This is most clearly seen in Figure 4 for $\alpha k = 0.5$.) All such solutions eventually escape to infinity along $u \sim v \to -\infty$.

The numerical simulations shown in Figures 3-5 for $\alpha k = 0.3$, 0.5, and 0.95 were obtained by choosing a wide variety of initial conditions in the range $10^{-11} \leq u_0 \leq 10^{-7}$ and computing the corresponding initial values for v_0 from the Taylor series $v_0 = \phi(u_0)$. The number of time steps executed before blow-up was encountered (measured by $|u_n| + |v_n| > 100$) varied erratically from approximately 25 to 5,000 depending on the number of cycles performed around the centres.

Another interesting feature of the solutions of (2.11) is the transition from orbital solutions around the centres (1,0) and (0,1). The insets in Figures 4 and 5 show the appearance of islands (obtained by judicious choices of initial values (u_0,v_0)); during each cycle around the centre, one point is placed on each island. The 'centres' of these islands therefore constitute periodic solutions of (2.11), (period 7 for $\alpha k = 0.5$ and period 8 for $\alpha k = 0.95$) while the immediate exterior of the islands is part of the unstable manifold emanating from the origin.

As αk is increased beyond unity, the fixed points (0,1) and (1,0) are no longer centres and consequently orbits do not exist although there may still be periodic solutions.

2.3 Chaos via Hopf Bifurcation (Map in 4-space)

An alternate route to chaos, via Hopf bifurcation, is provided by the Adams predictor-corrector scheme

$$\begin{aligned} U_{n+1}^{(p)} &= U_n + \frac{k}{24}[55U_n(1-U_n) - 59U_{n-1}(1-U_{n-1}) + 37U_{n-2}(1-U_{n-2}) \\ &\qquad - 9U_{n-3}(1-U_{n-3})] \\ U_{n+1} &= U_n + \frac{k}{24}[9U_n^{(p)}(1-U_n^{(p)}) + 19U_n(1-U_n) - 5U_{n-1}(1-U_{n-1}) \\ &\qquad + U_{n-2}(1-U_{n-2})] \end{aligned} \tag{2.12}$$

where we have put $\alpha = 1$. Linearisation about $U = 1$ in the usual way produces the quartic equation

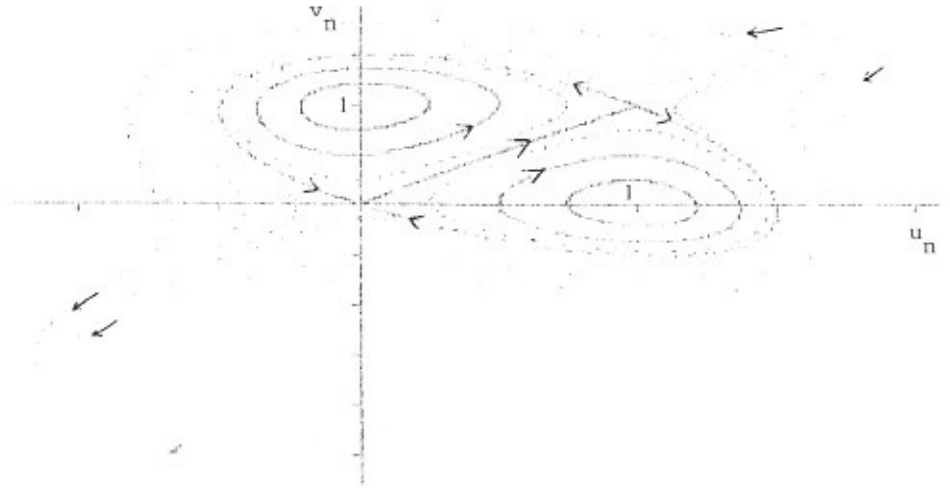

Figure 2 - Solutions of (2.11) for $\alpha k = 0.1$ from a variety of initial points (u_0, v_0).

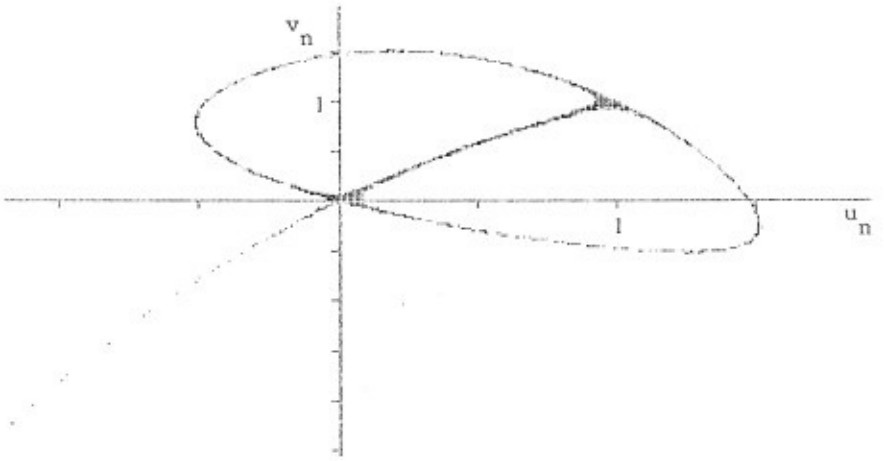

Figure 3 - Solutions of (2.11) for $\alpha k = 0.3$ and initial values $(u_0, \phi(u_0))$, $0 < u_0 \ll 1$.

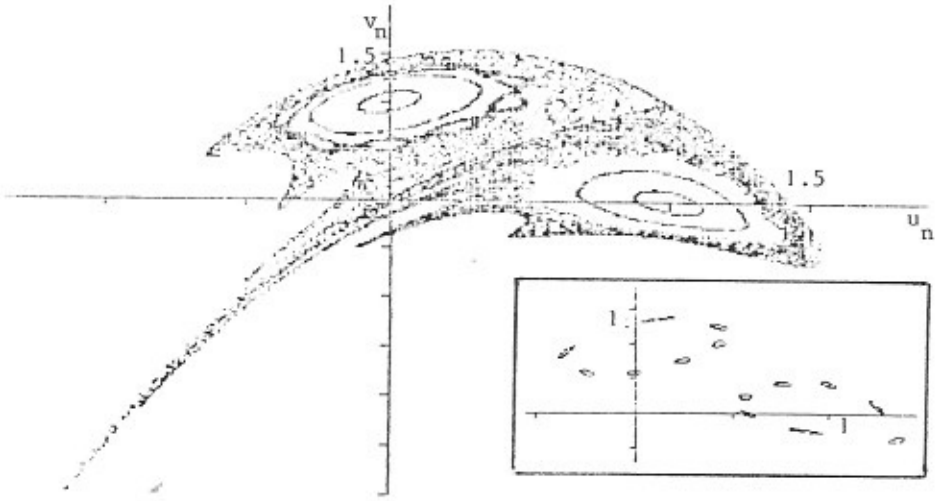

Figure 4 - Solutions of (2.11) for $\alpha k = 0.5$ with initial values i) $(u_0, \phi(u_0))$ $(0 < u_0 \ll 1)$ and ii) chosen to produce orbital solutions. The inset (reduced) shows the islands which exist in the transition zone between the image of the unstable manifold and the region of orbital solutions.

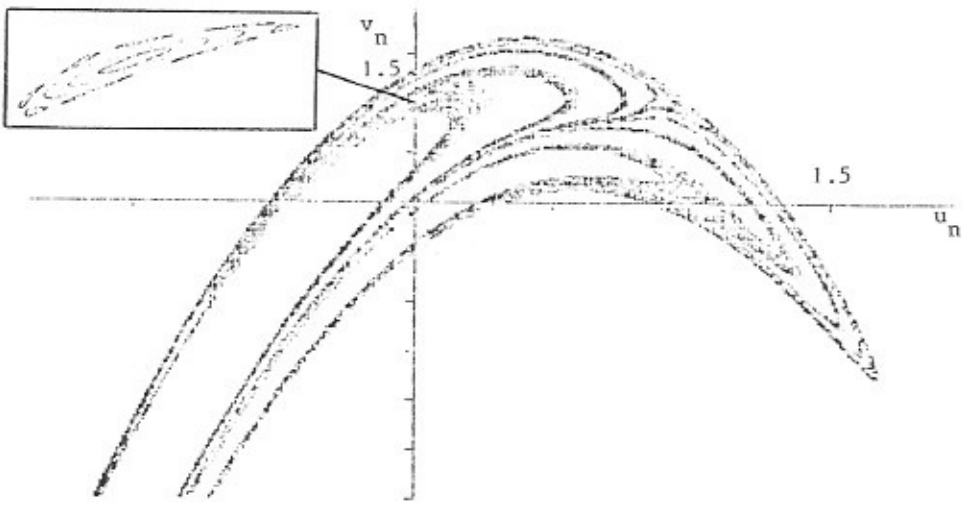

Figure 5 - Solutions of (2.11) for $\alpha k = 0.95$ and initial values $(u_0, \phi(u_0))$ $(0 < u_0 \ll 1)$. The inset shows the solutions in the neighbourhood of the centre (0,1).

$$\lambda^4 - (1 - \tfrac{7}{6}k + \tfrac{55}{64}k^2)\lambda^3 - (\tfrac{5}{24}k - \tfrac{59}{64}k^2)\lambda^2 + (\tfrac{1}{24}k - \tfrac{37}{64}k^2)\lambda + \tfrac{9}{64}k^2 = 0 \qquad (2.13)$$

for the amplification factor λ. The locations of the roots λ for the following values of k are as follows

$k = 0 \qquad \lambda = 1,0,0,0$

$k \doteqdot 1.28 \qquad \lambda \approx \cdot,\cdot,+i,-i$

$k = 8/3 \qquad \lambda = 1,1,1,1,$

where $\cdot$ signifies that the root is inside the unit circle in the complex plane. For the range $0 < k \leq \frac{8}{3}$ two of the roots are inside or on the unit circle whereas the other two roots are inside or on the unit circle for $0 < k < 1.28$ and outside the unit circle for $1.28 < k < 8/3$. Hopf bifurcation [5] occurs at $k \doteqdot 1.28$ and for $1.28 < k < 1.60$ (approximately) the attractors are invariant limit cycles. For $k > 1.60$, the limit cycles break down giving chaos via period doubling. Detailed calculations for $k > 1.28$ can be found in Prüfer [6].

2.4 Chaos in Reaction-Diffusion

We now study the effect on bifurcation of adding diffusion to (2.1) resulting in Fisher's equation with quadratic non-linearity

$$\frac{\partial u}{\partial t} = \alpha u(1-u) + \beta \frac{\partial^2 u}{\partial x^2}, \qquad \alpha,\beta > 0 . \qquad (2.14)$$

The forward Euler difference replacement of (2.14) is

$$U_m^{n+1} = U_m^n + \alpha k U_m^n(1-U_m^n) + \frac{\beta k}{h^2}(U_{m+1}^n - 2U_m^n + U_{m-1}^n) \qquad (2.15)$$

where $x = mh$ and $t = nk$, with m and n integers. A standard Von Neumann linearised stability analysis of (2.15) leads to the condition

$$0 \leq \alpha k(U_m^n - \tfrac{1}{2}) \leq 1 - \frac{2\beta k}{h^2}, \qquad (2.16)$$

and so adding diffusion appears to lower the linearised stability threshold.

We now carry out some numerical experiments where we choose a bifurcation free solution based on (2.1) with $a < 3$ and add diffusion to the problem by considering $\beta > 0$. Reverting to May's notation, (2.15) becomes

$$V_m^{n+1} = aV_m^n(1-V_m^n) + b(V_{m+1}^n - 2V_m^n + V_{m-1}^n) \qquad (2.17)$$

where $a = 1 + \alpha k$ and $b = \frac{\beta k}{h^2}$. The problem investigated is (2.17) subject to the initial condition

$$V(x,0) = \begin{cases} 0.5 & x = 0 \\ 0 & 0 < x \leq 100 \end{cases}$$

and the boundary conditions

$$\frac{\partial V(0,t)}{\partial x} = 0 \qquad \forall\ t > 0$$

$$V(L,t) = 0 \qquad \forall\ t > 0$$

where L is sufficiently large so as not to affect the results near $x = 0$. The numerical results obtained with $h = 0.5$, $k = 0.125$, $L = 100$ are given for $a = 2.915$ and increasing b as follows

b	V_0^n
$0 \leq b \leq 0.01$	0.65694683
$0.0125 \leq b \leq 0.1275$	Periodic
$0.1300 \leq b \leq 0.2150$	Chaos
$0.2150 < b$	Overflow

where for each value of b, up to 10,000 time steps were required to obtain the behaviour of the solution for large time. Further experimental corroboration of the destabilising effect of diffusion is available in Mitchell and Bruch [7].

3. NON-LINEAR DISPERSIVE WAVES

3.1 The Korteweg-de-Vriès (K.d.V.) equation

We consider next the KdV equation

$$\frac{\partial u}{\partial t} + u\frac{\partial u}{\partial x} + \varepsilon \frac{\partial^3 u}{\partial x^3} = 0 , \qquad \varepsilon > 0 . \tag{3.1}$$

For the linearised version of (3.1)

$$\frac{\partial u}{\partial t} + U \frac{\partial u}{\partial x} + \varepsilon \frac{\partial^3 u}{\partial x^3} = 0 , \qquad U \text{ constant},$$

periodic wavetrain solutions are given by

$$u = ae^{i(kx-wt)} \tag{3.2}$$

where a is the amplitude, k the wave number, and w the frequency, and

the dispersion relation is

$$w = k(U - \varepsilon k^2) \ .$$

For the nonlinear equation (3.1), however, (3.2) is not a solution and the dispersion relation, if it could be found, would involve the amplitude. Further details of dispersive waves can be found in the excellent treatise by Whitham [8].

3.2 Stability of the KdV equation

In order to examine the stability of the KdV equation we consider a small perturbation $\delta(x,t)$ on the solution $u(x,t)$ leading to the perturbation equation

$$\delta_t + u\delta_x + u_x\delta + (\tfrac{1}{2}\delta^2)_x + \varepsilon\delta_{xxx} = 0 \ . \tag{3.3}$$

Multiply (3.3) by δ and integrate with respect to x over a finite space interval I. For periodic boundary conditions, we obtain the result

$$\frac{d}{dt}\| \delta(t) \|_{L_2}^2 + \int_I \delta^2(x,t) \frac{\partial u(x,t)}{\partial x} \, dx = 0 \ . \tag{3.4}$$

If $\frac{\partial u}{\partial x} < 0$, then $\frac{d}{dt}\| \delta(t) \|_{L_2}^2 > 0$ and so $\delta(t)$ increases and it would appear that a negative gradient in the initial condition for example would trigger off an instability in the solution of (3.1). Thus although the zero dispersion limit for the KdV equation is complicated (Lax [9]) it would appear that this result is consistent with the appearance of a shock due to converging straight characteristics when $\varepsilon = 0$ and a negative gradient is present in the initial condition.

3.3 Discretisation in Space

Using equally spaced finite elements with piecewise linear basis functions the nonlinear term gives either

$$u \frac{\partial u}{\partial x} \sim \frac{1}{3}(U_{m+1} + U_m + U_{m-1}) \frac{1}{2h}(U_{m+1} - U_{m-1}) \sim \frac{1}{2}\frac{\partial}{\partial x}(u^2)$$

for the standard Galerkin method where $u \sim U = \sum_i U_i \phi_i(x)$ or

$$\frac{1}{2}\frac{\partial}{\partial x}(u^2) \sim \frac{1}{2}(U_{m+1} + U_{m-1}) \frac{1}{2h}(U_{m+1} - U_{m-1}) = \frac{1}{4h}(U_{m+1}^2 - U_{m-1}^2)$$

for product approximation [10] where $u^2 \sim U^2 = \sum_i U_i^2 \phi_i(x)$. The mass matrix is formed from

$$u \sim U = \frac{1}{6}\,(U_{m+1} + 4U_m + U_{m-1}) = (1 + \frac{1}{6}\,\delta^2)U_m$$

where δ is the central difference operator.

With finite differences, the nonlinear term is written in the form

$$\theta \frac{\partial}{\partial x}\,(\tfrac{1}{2}u^2) + (1-\theta)u\,\frac{\partial u}{\partial x}\,, \qquad 0 \le \theta \le 1$$

and using central differences we obtain the finite element formulae above when

$\theta = 2/3$ Standard Galerkin

$\theta = 1$ Product Approximation

There are many possible finite element representations of the dispersion term, but in finite differences we always use

$$\frac{\partial^3 u}{\partial x^3} \sim \frac{1}{2h^3}\,[U_{m+2} - 2U_{m+1} + 2U_{m-1} - U_{m-2}]$$

3.4 Linearised Stability of Difference Schemes

We now carry out a standard Von Neumann stability analysis on the linearised forms of the various space and time discretisations of the KdV equation. Note that the linearisations do not involve the parameter θ. If E_m^n is the error in U_m^n where

$$E_m^n \sim e^{\gamma nk} e^{i\delta mh}, \qquad \gamma,\delta \text{ constants}$$

the Von Neumann condition is

$$|e^{\gamma k}| \le 1\,. \tag{3.5}$$

If we put $A = \sin\phi(\alpha - 4\beta\sin^2\frac{\phi}{2})$ with $\phi = \delta h$, $\alpha = \frac{Uk}{h}$, $\beta = \frac{\varepsilon k}{h^3}$, where U is the constant solution about which the linearisation is performed we get the following results for the various time-stepping procedures.

Euler $|e^{\gamma k}| = \sqrt{1 + A^2}$ All modes unstable

Leap Frog $e^{\gamma k} = -iA \pm \sqrt{1 - A^2}$

(i) $A^2 \le 1$ Modes neutrally stable

(ii) $A^2 > 1$ Modes unstable

Crank-Nicolson $e^{\gamma k} = \frac{1 - 2iA}{1 + 2iA}$ All modes neutrally stable

3.5 Nonlinear Stability of Difference Schemes

Here the only results are for

$$\frac{\partial u}{\partial t} + \theta \frac{\partial}{\partial x}(\tfrac{1}{2}u^2) + (1-\theta)u \frac{\partial u}{\partial x} = 0 \qquad (\varepsilon = 0)$$

where for central differences in space, Fornberg [11] has shown that $\theta = 2/3$ is necessary for stability of leap frog and necessary and sufficient for stability of Crank Nicolson. Stability here means that the L_2 norm of the difference approximation does not increase faster in time than a fixed exponential function even if the mesh is refined.

3.6 Numerical Studies and Recurrence

The pure initial value problem for the KdV equation where solutions tend to zero rapidly as $|x|$ tends to ∞ causes no great problem numerically. In these problems after the elapse of some time, solitary waves (solitons) appear, each of which propagates with a fixed speed and unaltered shape. Analytically this problem can be solved by inverse scattering theory for potentials vanishing at $x = \pm\infty$ [12]. The initial value problem for solutions which are periodic in x is much more difficult theoretically and numerically, however, and this is the problem on which we carry out numerical tests. The initial numerical steps in this problem were taken by Zabusky and Kruskal [13] who observed that solutions with sinusoidal initial values developed into wave patterns which eventually reverted to a resemblance of the initial shape. These solutions periodic in space and almost periodic in time were more or less confirmed theoretically by Lax [14].

For our numerical experiments we choose the initial condition

$$u(x) = \cos 2\pi x , \qquad 0 \le x \le 1,$$

and periodic boundary conditions at $x = 0,1$ for $t > 0$. Since $\frac{\partial u}{\partial x} < 0$ for $0 < x < \frac{1}{2}$ at $t = 0$, instabilities were expected to appear initially and in order that these be not suppressed artificially, the explicit leap frog scheme with unstable and neutrally stable modes was used. A typical numerical experiment shows the sinusoidal initial condition developing a perturbation close to $x = \frac{1}{4}$ which grows into a wave pattern and then reverts to an approximation of the initial condition. This phenomenon is known as recurrence.

4. FOURIER ANALYSIS AND NON LINEAR INTERACTIONS

We consider a time dependent problem (e.g. KdV) with one space variable and periodic boundary conditions. The unit interval is divided equally by the points $x = mh$, $m = 0,1,\ldots,M$. The numerical solution at time t transforms into discrete Fourier space as

$$U_m(t) = \sum_{p=-M/2}^{+M/2} a_p(t) e^{2\pi i p \frac{m}{M}}, \tag{4.1}$$

where $|p| \leq M/2$ is the wave number and M is even. From (4.1), we see that quadratic interactions lead to terms of the form

$$e^{2\pi i p_1 x} \; e^{2\pi i p_2 x} = e^{2\pi i (p_1 + p_2) x}$$

and if $p_1 + p_2 > M/2$, the newly formed mode is incorrectly represented as $p_1 + p_2 - M$, a phenomenon referred to as aliasing. That is, there is a transfer of energy from the mode with wavenumber $p_1 + p_2$ to that with wavenumber $p_1 + p_2 - M$.

4.1 Reduction of Dimension of Problem

The non linear interactions mentioned above can only be followed realistically when a small number of Fourier components is involved. For example, the problem with periodic boundary conditions and period M in space has the solution form

$$U(mh,t) = a(t)\sin\frac{2\pi m}{3} + b(t)\cos\frac{2\pi m}{3} + c(t) \qquad m = 0,1,2,\ldots \tag{4.2}$$

when $M = 3$, and

$$U(mh,t) = a(t)\sin\frac{\pi m}{2} + b_1(t)\cos\frac{\pi m}{2} + b_2(t)\cos \pi m + c(t) \qquad m = 0,1,2,3,\ldots \tag{4.3}$$

when $M = 4$.

The KdV equation is now written in the form

$$\frac{\partial u}{\partial t} + \theta \frac{\partial}{\partial x}(\tfrac{1}{2}u^2) + (1-\theta)u\frac{\partial u}{\partial x} + \varepsilon \frac{\partial^3 u}{\partial x^3} = 0, \qquad 0 \leq \theta \leq 1, \; \varepsilon > 0$$

and discretisation in space using central differences for the middle two terms leads to

$$\frac{\partial U}{\partial t} + \frac{1}{2h}(U_{m+1} - U_{m-1})[\tfrac{1}{2}\theta(U_{m+1} + U_{m-1}) + (1-\theta)U_m] + \frac{\varepsilon}{2h^3}[U_{m+2} - 2U_{m+1} + 2U_{m-1} - U_{m-2}] = 0 \tag{4.4}$$

Substitution of (4.2) into (4.4) leads to the 3-system

$$\begin{aligned}
\frac{da}{dt} &= \frac{\sqrt{3}}{4h}\,(1-\tfrac{3}{2}\theta)(a^2-b^2+2bc) - \varepsilon\,\frac{3\sqrt{3}}{2h^3}\,b \\
\frac{db}{dt} &= -\frac{\sqrt{3}}{2h}\,(1-\tfrac{3}{2}\theta)a(b+c) + \varepsilon\,\frac{3\sqrt{3}}{2h^3}\,a \\
\frac{dc}{dt} &= 0
\end{aligned} \tag{4.5}$$

and substitution of (4.3) into (4.4) leads to the 4-system

$$\begin{aligned}
\frac{da}{dt} &= \frac{1}{h}\,b_1[2\theta b_2-(b_2-c)] - \frac{2\varepsilon}{h^3}\,b_1 \\
\frac{db_1}{dt} &= \frac{1}{h}\,a[2\theta b_2-(b_2+c)] + \frac{2\varepsilon}{h^3}\,a \\
\frac{db_2}{dt} &= -\frac{1}{h}(1-\theta)ab_1 \\
\frac{dc}{dt} &= 0\ .
\end{aligned} \tag{4.6}$$

Systems similar to (4.5) and (4.6) were obtained by Briggs et al [15] for the case $\varepsilon = 0$. It should be noted that $\theta = \frac{2}{3}$ linearises the system (4.5) and $\theta = 1$ the system (4.6). Also (4.6) with $\varepsilon = 0$ and $\theta = 1$ appears on pp. 128, 129 of Richtmyer and Morton [16] as an example of a system which for appropriate initial conditions becomes unstable in time. If it were possible to solve the above semi-discrete systems exactly, no new modes would be introduced since aliasing projects modes formed by non linear interactions back on to one or other of the original modes. The amplitudes of the original modes then depend on the initial condition together with non linear interactions and aliasing.

Theoretical and numerical studies of systems (4.5) and (4.6) are being carried out at present.

4.2 Round-off Errors and Side Bands

The semi-discrete systems are now discretised in time by the leap frog scheme (mid point rule). It is unlikely that the nonlinear partial difference equations obtained will ever be solved exactly and so we resort to numerical methods. The introduction of round-off errors may of course lead to a focusing mechanism for the destabilisation of the nonlinear difference schemes, a phenomenon discussed in the important paper by Briggs et al [15]. We now relate this mechanism for the triggering of nonlinear instabilities to

the disintegration of periodic wavetrains on deep water analysed in a classic paper by Benjamin and Feir [17]. To quote from the latter, consider a periodic wavetrain given by

$$u = ae^{i\zeta}, \quad \zeta = kx - wt \ , \tag{4.7}$$

leading to

$$u \frac{\partial u}{\partial x} = a^2 k i e^{2i\zeta} \ ,$$

the second harmonic of the primary wave. Higher harmonics lead to amplitudes

$$a^3k^2, \ a^4k^3, \text{ etc.},$$

which decrease only if a is small. Now consider side band modes to the primary mode of wave number k given by

$$\zeta_1 = (k+\mu)x - (w+\delta)t - \gamma_1 \qquad [\varepsilon_1]$$

and

$$\zeta_2 = (k-\mu)x - (w-\delta)t - \gamma_2 \qquad [\varepsilon_2]$$

where $[\varepsilon_1]$ and $[\varepsilon_2]$ are the respective small amplitudes. A simple calculation gives

$$\zeta_1 + \zeta_2 - 2\zeta = -(\gamma_1 + \gamma_2)$$

and so if

$$\gamma_1 + \gamma_2 = \text{constant},$$

called the resonance condition, the pair of side bands feed each other leading to nonlinear instability. Numerical experiments conducted by David Sloan [18] on $\frac{\partial u}{\partial t} + u \frac{\partial u}{\partial x} = 0$ show that the growth rate of a side band mode varies with the separation, in wave number space, between either side band and the primary mode.

In conclusion it should be stated that although there is a strong connection between round-off errors and side band modes, (4.7) is a solution of the KdV equation only after it has been linearised.

REFERENCES

1. MAY, R.M. Simple mathematical models with very complicated dynamics, Nature 261 (1976) 459-467.

2. FEIGENBAUM, M.J. The metric universal properties of period doubling bifurcations, Nonlinear dynamics (ed. R.H.G. Helleman), Annals N.Y. Acad. Sci. 357 (1980) 330-336.

3. HÉNON, M. A two-dimensional mapping with a strange attractor, Comm. Math. Phys. 50 (1976) 69-77.

4. SANZ-SERNA, J.M. Studies in numerical nonlinear instability I. Why do leapfrog schemes go unstable?, SIAM J. SCI. STAT. COMPUT. 6 (1985) (in the press).

5. HOPF, E. Bifurcation of a periodic solution from a stationary solution of a differential system, Ber. Math. Phys. Sachsische Acad. Wissensch. (Leipzig) 94 (1942) 1-22.

6. PRÜFER, M. Turbulence in Multistep methods for initial value problems, SIAM J. Appl. Math. 45 (1985) 32-69.

7. MITCHELL, A.R. and BRUCH, J.C. Jr. A numerical study of chaos in a reaction diffusion equation, Num. Meths. for P.D.Es. 1 (1985) 13-23.

8. WHITHAM, G.B. Linear and Nonlinear Waves, John Wiley and Sons, London, 1974.

9. LAX, P.D. and LEVERMORE, C.D. On the small dispersion limit for the KdV equation, Comm. Pure Appl. Math. 36, (1983) 253-290.

10. CHRISTIE, I., GRIFFITHS, D.F., MITCHELL, A.R. and SANZ-SERNA, J.M. Product approximation for nonlinear problems in the finite element method, IMA Journ. of Num. Anal. 1 (1981) 253-267.

11. FORNBERG, B. On the instability of leap-frog and Crank-Nicolson approximation of a non-linear partial differential equation, Math. Comp. 27 (1973) 45-57.

12. ZAKHAROV, V.E. and SHABAT, A.V. Exact theory of two-dimensional self-focusing and one dimensional self-modulation of waves in nonlinear media, Zh. Eksp. Tear. Fiz. 61 (1971) 118.

13. ZABUSKY, N.J. and KRUSKAL, M.D. Interaction of "solitons" in a collisionless plasma and the recurrence of initial states, Phys. Rev. Lett. 15 (1965) 240-243.

14. LAX, P.D. Periodic solutions of the KdV equation, Comm. Pure Appl. Maths. 28 (1975) 141-188.

15. BRIGGS, W., NEWELL, A.C. and SARIE, T. Focusing: A mechanism for instability of nonlinear finite difference equations, J. Comp. Phys. 51 (1983) 83-106.

16. RICHTMYER, R.D. and MORTON, K.W. Difference Methods for Initial Value Problems, John Wiley and Sons, New York, 1967.

17. BENJAMIN, T.B. and FEIR, J.E. The disintegration of wave trains on deep water, J. Fluid. Mech. 27 (1967) 417-430.

18. SLOAN, D.M. and MITCHELL, A.R. On nonlinear instabilities in leap-frog finite difference schemes, Num. Anal. Rep. NA/87, Univ. of Dundee, 1985.

A.R. Mitchell & D.F. Griffiths
Department of Mathematical Sciences
University of Dundee
Dundee DD1 4HN
Scotland
U.K.